Available online at www.sciencedirect.com

ScienceDirect

Energy Procedia 53 (2014) 104 – 113

Energy Procedia

EERA DeepWind'2014, 11th Deep Sea Offshore Wind R&D Conference

Experimental verification of a voltage droop control for grid integration of offshore wind farms using multi-terminal HVDC

Raymundo E. Torres-Olguin[a], Atle R. Årdal[a], Hanne Støylen[b] , Atsede G. Endegnanew[ab], Kjell Ljøkelsøy[a], John Olav Tande[a]

[a]SINTEF Energy Research, Sem Sælands vei 11, 7465 Trondheim, Norway
[b]NTNU dept. of Electric Power Engineering, O.S Bragstads plass 2E, 7034 Trondheim, Norway

Abstract

This paper presents an experimental verification of a voltage droop control for a multi-terminal HVDC system for the grid integration of offshore wind farms. The laboratory setup is composed by four voltage-source converter terminals which aim to emulate behavior of the future power grid in the North Sea, where Norway, Germany and the UK are interconnected together with an offshore wind farm. Two main scenarios have been performed to test the robustness of the droop-control strategy: variation in wind power, including changes in the parameters of the droop line, and the sudden disconnection of converter terminal during full wind production. In all performed cases, the implemented system was able to ensure that the voltage stays within its steady state limits and to reach a stable operation point.

Selection and peer-review under responsibility of SINTEF Energi AS

Keyword:North sea super grid; multi-terminal HVDC; droop voltage control.

1. Introduction

In the near future, the construction of an offshore electrical grid is expected in Europe [1]. The objective of such a transmission infrastructure, which is called North Sea Super-grid (NSSG), is to facilitate large-scale integration of renewable energy and to improve the European power market. One of the greatest challenges in the realization of the NSSG is the long-distance bulk-power delivery. It is widely recognized that HVDC transmission is more economically attractive than HVAC transmission [2]. Therefore, HVDC is considered the better choice for the NSSG. Moreover, it is assumed that voltage-source converters (VSCs) will be used since the traditional line-commutated converters (LCC) are not suitable for multi-terminal HVDC systems.

Selection and peer-review under responsibility of SINTEF Energi AS
doi:10.1016/j.egypro.2014.07.219

A multi-terminal HVDC system presents many challenges. Among these challenges are: protection [3-5], control [6, 7], and operation [7, 8] issues. One of the most critical issues is voltage control and power balancing [7]. Precise and automated control of voltage enables possibilities for power balancing between terminals. Several methodologies to balance the power and control the voltage have been studied in the literature:

One approach is to use a centralized approach, where one power converter controls the DC voltage. For instance, in *Master-Slave control,* which is an extension of the conventional point-to-point control, only one terminal controls the DC voltage (master-node/slack bus) and the rest control the power flow (slave-nodes [9] [10]). The voltage-power characteristic with the master-node, horizontal line, and slave-nodes, vertical line, is shown in Figure 1 a). Although master-slave control is easy to implement in a system, such centralized solution has many disadvantages, e.g. DC slack convert must be oversized; and system reliability may be compromised in the event of an outage of the DC slack converter [11]. In *Voltage-Margin control,* the slave-nodes are assigned a constant power region for a given voltage range and a constant voltage for any voltage outside this range [10, 12]. The relation between voltage and power for the slave-nodes is shown in Figure 1 b). However, in steady-state, it is still the master-node that is responsible for balancing the power. Thus, the master-node may still be subjected to large strains. Also, this approach may impose large instability issues on the AC grid as the power transfer to the converter may change fast with large increments.

Another approach is to distribute the DC voltage control to more than one converter. There are several possibilities such as: voltage droop control, dead-band voltage droop and undead-band voltage droop control. In *Voltage-Droop control,* each terminal is assigned a linear relationship between its DC voltage and the power flowing through its terminals, see Figure 1c). In this way, the terminals share the task of maintaining the system voltage as well as the duty of instantaneous power balancing in the power grid [3]. *Dead-band and undead-band droop control* are combinations of the voltage margin and voltage droop control strategies. For the dead-band droop control, the terminal is a constant power node for a given voltage range, but for any voltage outside this range a droop is given as shown in Figure 1 d). This allows discriminating between normal and disturbed operation. For the undead-band droop control, the relation between voltage and power is always linear, but the droop constant differs for normal and disturbed operation

Full scale experiments provide the most reliable results, but may not be feasible due to economic and safety issues. Laboratory experiments on scaled down physical models are a better alternative to reduce costs, size and risks. A down-scaled model is used in this paper in order to replicate the behavior of the full size HVDC system. Moreover, in order to control the DC voltage and sharing the power, this paper is focused on the verification of a droop-based voltage control. This voltage droop control scheme is an attractive option since it only depends on local measurements, i.e. it does not need fast communications between the terminals. Although this concept has been studied extensively in the literature, few works have showed experimental results [13, 14]. The scope of this work is limited to primary control. Secondary control, such as restoring the nominal DC voltage or achieving the desired level of power flow at certain converter terminal, is not considered part of this work.

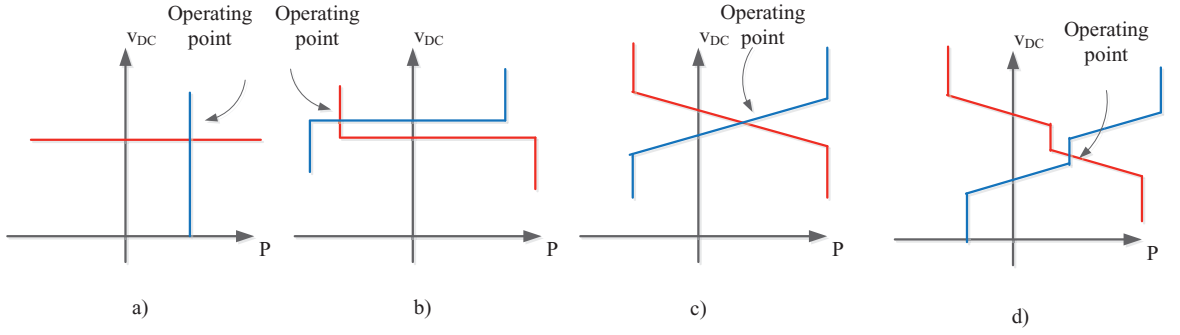

Figure 1 P-V characteristics of voltage and power control methods for MTDC grids. a) master/slave mode b) voltage margin control c) DC droop control d) dead-band droop control

2. Reference system

The system under study is a multi-terminal HVDC system composed of four terminals. The terminal named VSC_W connects the offshore wind farms and the other terminals connect three different onshore grids as shown in Figure 1. VSC_W injects the power generated in the wind farms, while VSC_{NO}, VSC_{GE} and VSC_{UK} can import or export power from the HVDC into the respective main grids. The voltage control and power balance of such of multi-terminal HVDC system is performed using a voltage droop controller. In this hypothetical case, it is assumed that the three onshore grids have a nominal voltage of 400 kV. Each converter and cable is rated at 1200 MW at ± 320 kV. A 1200 MW offshore wind farm with VSC supplies the HVDC system. The distances between VSC_{NO}, VSC_{GE} and VSC_{UK}, and the common node O are 600, 300 and 200 respectively. The main parameters are listed in Table 1.

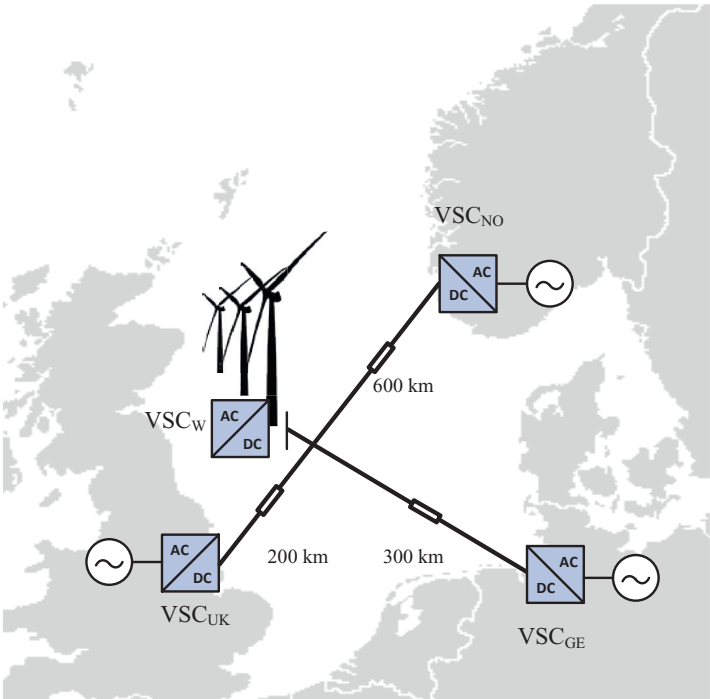

Figure 2 A schematic diagram which illustrates the multi-terminal system

Table 1 System parameters

Parameter	Value	Unit
Onshore base voltage	400	kV
HVDC power rating	1200	MW
HVDC pole-to-pole DC voltage	640	kV
Wind farm	1200	MW
Cable length	200, 300, and 600	km

3. Multi-terminal laboratory set-up

An experimental platform has been configured at the SINTEF/NTNU Renewable Energy Systems Laboratory in order to verify the droop voltage controller and emulate the behaviour of the system described in Figure 2. The set-up consists of four VSCs connected in the DC side using a DC line emulator. The wind farm is emulated using a 55 kVA induction generator which is driven by an induction motor in order to represent the wind behaviour. The emulated wind farm is directly connected to the one of the VSCs. The grids are simply obtained by connecting to the 400 V main grid via three phase 1:1 transformers. The voltage source converters are rated to 60 kVA. The whole device is composed by: converter, LCL smoothing filter, switchgear, and the control system. The converters use two-level configuration based on insulated gate bipolar transistors (IGBTs) which is switching at 5 kHz. The grid connection is through a LCL filter with the following parameters: converter-side filter inductor 50 μH, capacitor 20 μF and grid side filter inductor 200 μH. The scaling factors and the procedure how they were chosen are shown in Appendix A.

The control system runs on a processor system that is embedded in an FPGA (Field-Programmable Gate Arrays). The converters and the motor-drive are equipped with a control area network (CAN) interface which enables receiving status messages and measurements and sending control actions. The voltage droop control is achieved by using the LabVIEW^{TM} programming environment which specifies the reference signal using CAN communication. The DC line emulator consists of a set of series resistors with parallel switches with switches in order to vary the length of the emulated cable.

A schematic representation of the experimental platform is shown in Figure 3, and a photo of the setup is shown in Figure 9 located in Appendix A.

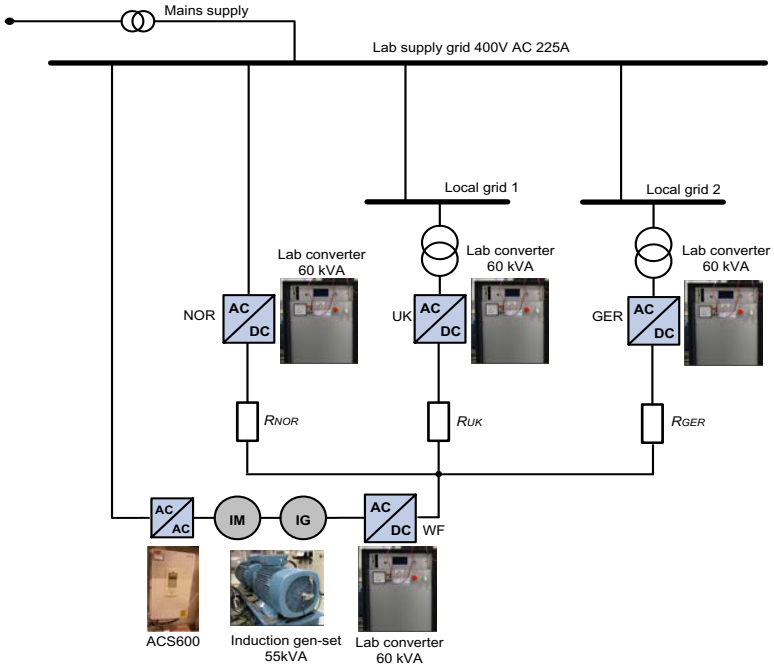

Figure 3 Experimental platform of MTDC system

4. Implementation of voltage droop controller

Voltage droop control scheme is based on the strategy implemented in traditional AC systems where the frequency is used as indicator to adjust the generated power. In MTDC systems, the indicator is the DC voltage which is used to adjust the current at the converters and consequently it is possible to regulate the DC voltage in the MTDC system

[11]. In this work, the control strategy applied to the power converters is the well-known vector control which consists of a cascaded control structure with one inner and one outer control loop. The inner loop regulates the currents in a synchronous reference frame maintained by a phase locked loop, and the outer loop is different for the converters when they are connected directly to a grid or integrates an offshore wind farm. For grid connected converters, a voltage-droop control scheme is applied, whereas the wind farm connected converter is always delivering the available power (slave-node) since the power flow is governed by the generator speed. The droop control is a simple proportional control that regulates the dc voltage and provides power sharing between different converters [13]. The mathematical expression for voltage droop control is given by

$$V_{DC}^{*} = V_0 - \rho(P_{DC} - P_0) \tag{1}$$

where V_{DC}^{*} and P_{DC} are the DC voltage and power in the converter, V_0 and P_0 are the voltage and power set-points, and ρ is the droop constant. This expression forms the droop line and the control system objective is to force the converter to have an operating point on the droop line.

Typically, voltage droop control is implemented directly acting on the inner current control loop [13]. In this paper, the voltage droop controller acts directly on the DC voltage reference. The block diagram in Figure 4 shows how the droop is implemented in the set up. The inner current control is represented as a first order response with an equivalent time constant T_{eq}. The reference for the inner loop is obtained using a PI controller, which is called DC voltage control in Figure 4, where K_{pv} and T_{iv} represent the proportional gain and integral time respectively. There are some practical issues to consider when implementing the DC voltage droop. Firstly, there is a time delay of approximately 10 ms due to the sampling time of the communication between the converters and LabVIEW™ program. Secondly, real measurements of the power flowing through the DC terminals of the converters were not available with the present version of the converter control system. Instead, the d-axis current is used, based on the assumption that the active power on the AC side is proportional with the d-axis current. The measured d-axis current is multiplied with a calibration constant in order to convert the current to power. The measured "power" is then subtracted from the power set point and divided with the droop constant. Adding the voltage set-point generated the DC voltage reference value, which is sent through the CAN bus and received by the converter.

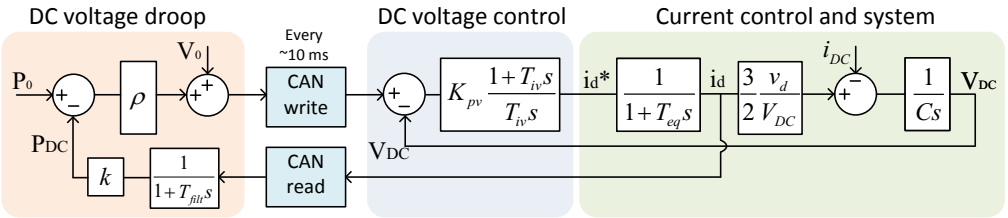

Figure 4 Block diagram of the implemented DC voltage droop control

5. Experimental results

Two main case studies are defined to investigate if the voltage droop control will ensure stable operation in a real MTDC grid.

Case 1: Variation of the wind production with three subcases:
- Case 1 a) equal droop constants and power set points
- Case 1 b) equal power set points and unequal droop constants
- Case 1 c) equal droop constants and unequal power set points.

Case 2: Loss of two terminals during full wind production

Figure 5 shows the voltages and powers at the DC side of each converter when the wind power production varies. At the beginning from 5 to 10 s, the wind power production is set at zero and the reference voltages are displayed in Figure 5. At t=10 s, the wind power starts to increase using an up ramp function which emulates the wind behaviour, consequently, the voltages of the DC grid start to rise according to the voltage droop controller described in (1). At t= 35 s, the power from the wind farm decreases using a down ramp function, and the voltage of the DC grids falls as expected as is illustrated in Figure 5. The droop parameters for all the converters are: V_0 = 640 V, P_0 = 0 kW and ρ = 20 power pu/voltage pu.

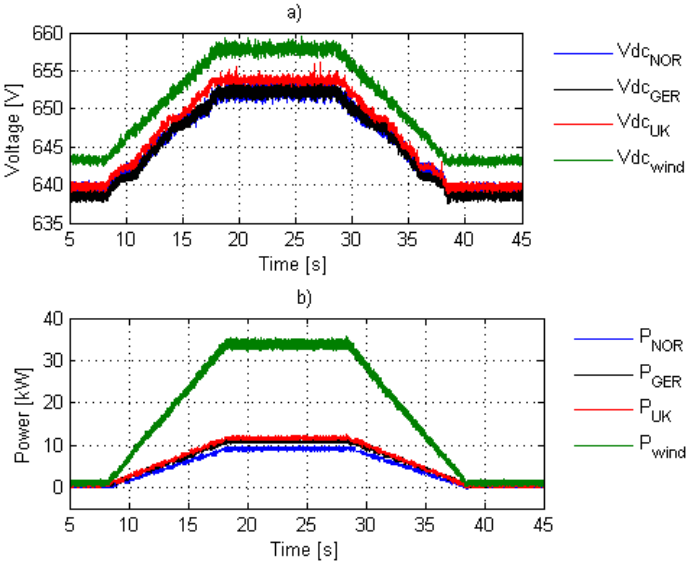

Figure 5 Experimental results for the case with varying wind power. a) voltages and b) powers for the multi-terminal HVDC system under study.

The above experimental results show that the produced power from the wind farm is shared equally between the three countries. This is because their respective droop lines have identical voltage and power set-points, and identical droop-line constants, see equation (1). Figure 6 shows the system response to wind power changes using the up and down ramp function; however, the droop constants have been chosen to distribute the wind power proportional to the value of the droop constants. The set-points are: V_0 = 640 V and P_0 = 0 kW for all the converters, and different droop constants: 20 (Norway), 40 (Germany) and 10 (UK) power pu/voltage pu. The powers are distributed proportionally to the droop constants, so Germany gets about twice the power flow of Norway, and so on. The voltages change according to the droop controller law to meet their respective equilibrium points as shown in Figure 6. Figure 7 shows the system response to wind power changes using the using an up and down ramp function but the power set-point has been modified: - 0.5 pu (Norway), 0.25 pu (Germany) and 0.25 pu (UK). Figure 7 shows how the power is shifted according to the new power set-points, and the voltages change to reach their respective equilibrium points.

Figure 8 shows the case when there is a loss of two converters during high wind power production. The wind farm produces approximately 40 kW, at t=0.7 s the converter in Norway is disconnected. When Norway is disconnected the power is redistributed among the remaining two terminals. At t=1.7 s, the converter in UK is also disconnected and the converter in Germany takes the rest of the power as shown in Figure 8. In practice it is important to not exceed any limits in either the converters or DC cables e.g. in a real system the power rating of the DC cable between the wind farm and Germany might not be the same as the rating of the wind farm. It worth to mention that the noise in the curves, especially in the dc voltages, is caused by the combined effect of fairly high gain in the droop regulators and limited resolution in DC voltage measurement signals transferred over the CAN bus.

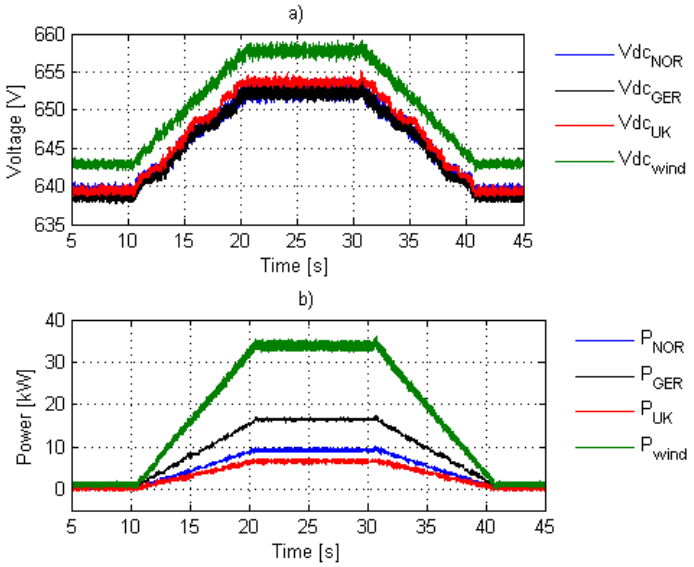

Figure 6 Experimental results for the case with varying wind farm power and unequal droop constant but equal set-points. a) voltages and b) powers for the multi-terminal HVDC system under study.

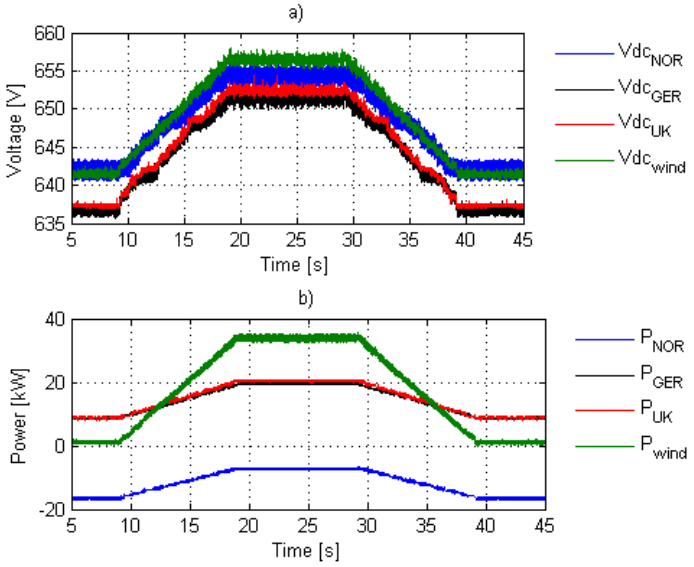

Figure 7 Experimental results for the case with varying wind farm power and equal droop constant and unequal set-points. a) voltages and b) powers for the multi-terminal HVDC system under study.

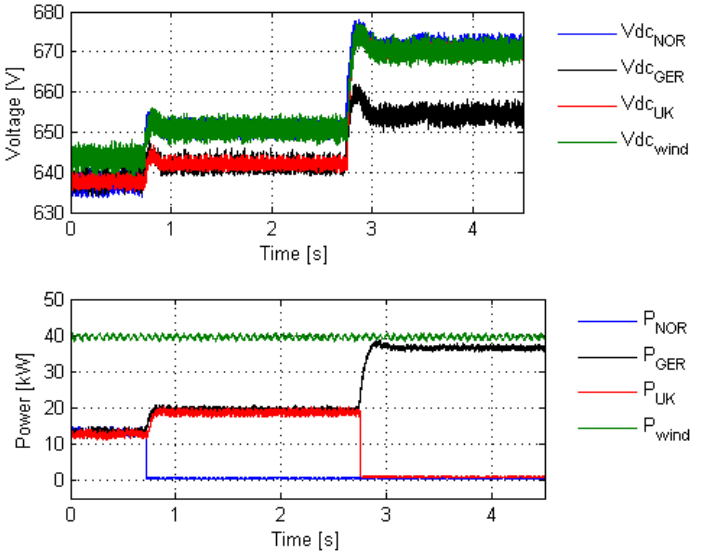

Figure 8 Experimental results for the case when loss of converter terminals during full wind production is analysed. a) voltages and b) powers for the multi-terminal HVDC system under study.

6. Conclusions

This work contributes to research on a four-terminal voltage-source converter high-voltage-direct-current system in the area of voltage-control and operation. The overall goal has been to implement a voltage droop control in a down scaled model of a multi-terminal VSC-HVDC grid. Two scenarios have been used to test the performance of the droop-control and evaluate the stability of the system: variation in wind power production including variation changes in droop line set-point parameters and loss of two terminals during full wind production. The implemented system was able to ensure that the voltage stays within its steady state limits and to reach a stable operation point after the above disturbances were applied. Moreover, the system is able to tolerate the loss of one or two terminals. It can be concluded that the voltage-droop control scheme has been successfully implemented in this laboratory model. However, special attention should be given to the delay in communications. Time delays give rise to phase lag which often degenerate system stability and performance, so they should be kept as short as possible.

For the future work, the following list summarizes suggested topics that could be investigated as part of future activities in NOWITECH

1. Wind farm connected to weak grid through MTDC network.
2. Exchange of frequency reserves between asynchronous AC-grids (primary and secondary reserves)
3. Provision of ancillary services (inertial response and primary frequency control) from offshore wind farms connected with HVDC or MT-HVDC.

Acknowledgements

This work has been supported by the Norwegian Research Centre of Offshore Wind Technology (NOWITECH)

Appendix A.

Below is described step by step in order to scale down for the multi-terminal system that was described in Figure 2.

1. Select a scaling factor for the power rating. The HVDC system between the onshore grids is rated at 1200 MW while the nominal power of the laboratory converters is 60 kVA. A 20 kVA load is connected to the synchronous generator so it can extract more power. The selection is based on trying to use the most power possible without compromising the laboratory equipment.. In this case chosen factor is 20 000, this means that 1200 MW is equivalent to 60 kVA.
2. Select a scaling factor for the voltage rating. The HVDC system is rated at 1200 MW at ± 320 kV and the system is connected to a 400 kV AC system. The main voltage level in the laboratory is 400 V. The natural choice for the scaling factor is 1000. This means that ± 320 kV and 400 kV are equivalent to 320 V and 400 V, in the MTDC system and the laboratory, respectively.
3. Select a scaling factor for the current rating. Since two base parameters have been chosen, the scaling factor for the current is automatically obtained, i.e. 20. This means that 1.875 kA in the MTDC system is the same as 93.75 in the laboratory platform.
4. Selecting a scaling factor for the cables. The HVDC system is connected through a long cable of 800 km and wind farm VSC is connected through a cable of 150 km. The rated voltage at the DC cable is ± 320 kV, so a cable with 2200 mm2 is assumed. The resistance of the cable R_{cable} is calculated as follows:

$$R_{cable} = \frac{\rho * l}{A} = \frac{1.68x10^{-8}\Omega m * 600\,000m}{0.0022m^2} = 4.58\Omega$$

where ρ is the copper density, l is the length of the cable and A is the cross section of the cable. We can calculate the power losses per unit using the resistance calculated above.

$$P_{losses,pu} = \frac{{i_N}^2 * R_{cable}}{P_N} = \frac{1.875\ kA^2 * 4.58\Omega}{1200\ MVA} = 1.34\%$$

where i_N is the nominal current and P_N is the nominal power in the MTDC.
In order to scale down the cable to the laboratory platform, the same power losses per unit should be used to calculate the resistance of the cable as follows.

$$P_{losses,pu} = \frac{{i_{N,lab}}^2 * R_{cable,lab}}{P_{N,lab}} = \frac{93.75^2 * R_{cable,lab}}{60kVA} = 1.34\%$$

where $i_{N,lab}$ is the nominal current and $P_{N,lab}$ is the nominal power in the laboratory set up. Solving for $R_{cable,lab}$

$$R_{cable,lab} = \frac{P_{N,lab} * P_{losses,pu}}{{i_{N,lab}}^2} = 91.5m\Omega$$

The same procedure in step 4 is used for the rest of the distances, i.e. 200 km and 300 km. The following table summarizes the scaling process:

Parameter	MTDC system	Lab set up	Scale factor
Power	1200 MVA	60 kVA	1:20000
DC voltage	±320 kV	±320 V	1:1000
AC voltage	400 kV	400 V	1:1000
DC current	1.875 kA	46.875 A	1:40
Cable resistance (200 km)	1.52 Ω	30.5 mΩ	Same power losses
Cable resistance (300 km)	2.29 Ω	42.81 mΩ	Same power losses
Cable resistance (600 km)	4.58 Ω	91.5 mΩ	Same power losses

Figure 9 Photo of the laboratory setup

References

[1] N. Fichaux and J. Wilkes, *Oceans of Opportunity: Harnessing Europe's Largest Domestic Energy Resource*: EWEA, 2009.

[2] L. Xu and B. R. Andersen, "Grid connection of large offshore wind farms using HVDC," *Wind Energy,* vol. 9, pp. 371-382, 2006.

[3] D. Van Hertem and M. Ghandhari, "Multi-terminal VSC HVDC for the European supergrid: Obstacles," *Renewable and sustainable energy reviews,* vol. 14, pp. 3156-3163, 2010.

[4] O. Gomis-Bellmunt*, et al.*, "Topologies of multiterminal HVDC-VSC transmission for large offshore wind farms," *Electric Power Systems Research,* vol. 81, pp. 271-281, 2011.

[5] W. Lu and B.-T. Ooi, "DC overvoltage control during loss of converter in multiterminal voltage-source converter-based HVDC (M-VSC-HVDC)," *Power Delivery, IEEE Transactions on,* vol. 18, pp. 915-920, 2003.

[6] L. Jun*, et al.*, "Control of multi-terminal VSC-HVDC transmission for offshore wind power," in *Power Electronics and Applications, 2009. EPE '09. 13th European Conference on*, 2009, pp. 1-10.

[7] E. Prieto-Araujo*, et al.*, "Methodology for Droop Control Dynamic Analysis of Multiterminal VSC-HVDC Grids for Offshore Wind Farms," *Power Delivery, IEEE Transactions on,* vol. 26, pp. 2476-2485, 2011.

[8] O. Gomis-Bellmunt*, et al.*, "Voltage–current characteristics of multiterminal HVDC-VSC for offshore wind farms," *Electric Power Systems Research,* vol. 81, pp. 440-450, 2011.

[9] D. Jovcic, "Interconnecting offshore wind farms using multiterminal VSC-based HVDC," in *Power Engineering Society General Meeting, 2006. IEEE*, 2006, p. 7 pp.

[10] T. M. Haileselassie and K. Uhlen, "Precise control of power flow in multiterminal VSC-HVDCs using DC voltage droop control," in *Power and Energy Society General Meeting, 2012 IEEE*, 2012, pp. 1-9.

[11] R. T. Pinto*, et al.*, "Comparison of direct voltage control methods of multi-terminal DC (MTDC) networks through modular dynamic models," in *Power Electronics and Applications (EPE 2011), Proceedings of the 2011-14th European Conference on*, 2011, pp. 1-10.

[12] T. K. Vrana*, et al.*, "A Classification of DC Node Voltage Control Methods for HVDC Grids," *Electric Power Systems Research,* 2012.

[13] A. Egea-Alvarez*, et al.*, "Experimental implementation of a voltage control for a Multiterminal VSC-HVDC offshore transmission system," in *Innovative Smart Grid Technologies (ISGT Europe), 2012 3rd IEEE PES International Conference and Exhibition on*, 2012, pp. 1-7.

[14] A. Egea-Alvarez*, et al.*, "Voltage control of multiterminal VSC-HVDC transmission systems for offshore wind power plants: Design and implementation in a scaled platform," 2013.